Title	Functional responses and adaptation of mesophilic microbial communities to psychrophilic anaerobic digestion
Author(s)	Gunnigle, Eoin; Nielsen, Jeppe L.; Fuszard, Matthew; Botting, Catherine H.; Sheahan, Jerome; O'Flaherty, Vincent; Abram, Florence
Publication Date	2015-10-27
Publication Information	Gunnigle, Eoin, Nielsen, Jeppe L., Fuszard, Matthew, Botting, Catherine H., Sheahan, Jerome, O'Flaherty, Vincent, & Abram, Florence. (2015). Functional responses and adaptation of mesophilic microbial communities to psychrophilic anaerobic digestion. FEMS Microbiology Ecology, 91(12). doi: 10.1093/femsec/fiv132
Publisher	Oxford University Press
Link to publisher's version	https://doi.org/10.1093/femsec/fiv132
Item record	http://hdl.handle.net/10379/15423
DOI	http://dx.doi.org/10.1093/femsec/fiv132

Functional responses and adaptation of mesophilic microbial communities to psychrophilic anaerobic digestion

Article *in* FEMS Microbiology Ecology · October 2015

DOI: 10.1093/femsec/fiv132

CITATIONS
7

READS
210

7 authors, including:

Eoin Gunnigle

15 PUBLICATIONS **288** CITATIONS

SEE PROFILE

Jeppe Lund Nielsen

Aalborg University

281 PUBLICATIONS **7,068** CITATIONS

SEE PROFILE

Matthew A Fuszard

University of St Andrews

20 PUBLICATIONS **163** CITATIONS

SEE PROFILE

Vincent O'Flaherty

National University of Ireland, Galway

173 PUBLICATIONS **4,060** CITATIONS

SEE PROFILE

FEMS Microbiology Ecology Advance Access published October 26, 2015

Functional responses and adaptation of mesophilic microbial communities to psychrophilic anaerobic digestion

Authors: Eoin Gunnigle[1,5], Jeppe L. Nielsen[2], Matthew Fuszard[3], Catherine H. Botting[3], Jerome Sheahan[4], Vincent O'Flaherty[1] and Florence Abram[5]*

[1]Microbial Ecology Laboratory, Microbiology, School of Natural Sciences, National University of Ireland, Galway, Ireland.

[2]Department of Chemistry and Bioscience, Aalborg University, Aalborg, Denmark.

[3]Biomedical Sciences Research Complex, Biomolecular Sciences Building, University of St. Andrews, North Haugh, St. Andrews, Fife KY16 9ST, United Kingdom.

[4]School of Mathematics, Statistics and Applied Mathematics, National University of Ireland, Galway, Ireland.

[5]Functional Environmental Microbiology, School of Natural Sciences, National University of Ireland, Galway, Ireland.

***Author for correspondence:**

Address: Microbiology, School of Natural Sciences, National University of Ireland, Galway, University Road, Galway, Ireland.

Tel: +353 (0) 91 492390

Fax: +353 (0) 91 494598

e-mail: florence.abram@nuigalway.ie

Key words: anaerobic digestion, metaproteomics, microbial phylogenetic diversity, methanogenesis, psychrophilic, MAR-FISH

Running title: Microbial functional responses to psychrophilic AD

ABSTRACT

Psychrophilic (<20°C) anaerobic digestion (AD) represents an attractive alternative to mesophilic wastewater treatment. In order to investigate the AD microbiome response to temperature change, with particular emphasis on methanogenic archaea, duplicate laboratory-scale AD bioreactors were operated at 37°C followed by a temperature drop to 15°C. A volatile fatty acid-based wastewater (composed of propionic acid, butyric acid, acetic acid, and ethanol) was used to provide substrates representing the later stages of AD. Community structure was monitored using 16S rRNA gene clone libraries, as well as DNA and cDNA-based DGGE analysis, while the abundance of relevant methanogens was followed using qPCR. In addition, metaproteomics, microautoradiography-fluorescence *in situ* hybridization and methanogenic activity measurements were employed to investigate microbial activities and functions. *Methanomicrobiales* abundance increased at low temperature, which correlated with an increased contribution of CH_4 production from hydrogenotrophic methanogenesis at 15°C. *Methanosarcinales* utilised acetate and H_2/CO_2 as CH_4 precursors at both temperatures and a partial shift from acetoclastic to hydrogenotrophic methanogenesis was observed for this archaeal population at 15°C. An up-regulation of protein expression was reported at low temperature as well as the detection of chaperones indicating that mesophilic communities experienced stress during long-term exposure to 15°C. Overall, changes in microbial community structure and function were found to underpin the adaptation of mesophilic sludge to psychrophilic AD.

INTRODUCTION

The natural process of cold anaerobic digestion (AD) can be harnessed for wastewater treatment and bioenergy production. The potential of psychrophilic anaerobic digestion has been widely demonstrated through comparable treatment efficiencies against traditional mesophilic setups (e.g. McKeown *et al*., 2012), therefore circumventing the corresponding heating costs carried by industries. Consequently, full-scale applications of psychrophilic AD have recently been developed (e.g. Bio-Terre Systems inc. Canada). A current limitation, however, resides in the lack of understanding of the microbial communities underpinning the process. Indeed methane content and effluent quality are at present the principal tools employed to monitor treatment efficiencies but this approach is insufficient in the context of optimal process design and performance (Ramirez *et al*., 2009). During the process of AD, after initial decomposition of complex organic material by hydrolytic and fermentative bacteria, substrates are provided for methanogenesis in the form of CO_2/H_2, acetate and C-1-compounds like methanol and trimethylamine (Thauer *et al*., 2008). Hydrogenotrophic methanogens have been found to increase in relative abundance during long-term psychrophilic operation (McKeown *et al*., 2009). Indeed, Zhang *et al*. (2012) recorded a >30-fold increase in this group (16S rRNA gene abundance) when AD operating temperature was dropped from 18°C to 5°C. Nevertheless, acetoclastic methanogens are also prominent in low-temperature biomass, primarily *Methanosaetaceae*-like organisms (Collins *et al*., 2005), with this microbial group known to be important for the formation and structure of well-functioning granular sludge (McKeown *et al*., 2012). Although the enumeration of methanogens during psychrophilic AD operation has provided insights into community dynamics (McKeown *et al*., 2009; Siggins *et al*., 2011a), inferring

functional relevance/roles from such data is challenging, with divergence between presence and function recorded for a variety of habitats (Burke *et al*., 2011; Bailey *et al*., 2013; Zhi *et al*., 2014). As such, the molecular mechanisms employed that facilitate sub-mesophilic function remain unclear with only few examples of function-driven approaches undertaken on psychrophilic AD microbial communities to date (Abram *et al*., 2011; Siggins *et al*., 2012; Gunnigle *et al*., 2015). Furthermore, the primary routes of methanogenic carbon flow under these process conditions are still unresolved, which represents a significant knowledge gap in the operation of psychrophilic AD systems.

Recent advances in molecular methodologies have provided a platform from which metabolically active microbial groups can be resolved; these include meta-omic approaches focusing on RNA- and protein-isolated fractions (Jansson *et al*., 2012; Muller *et al*., 2013; Abram 2015). Moreover, ecophysiological approaches, such as isotope tracer techniques, have facilitated discrete substrate uptake dynamics at a cellular level to be monitored (Nielsen and Nielsen, 2005; Nikolausz *et al*., 2007). These approaches linked with phylogenetic analysis hold great promise in unraveling complex trophic interactions and, as such, in improving our understanding of psychrophilic AD systems. In this study, an integrative approach was employed to characterise the temperature-mediated functional response of methanogenic groups present in replicate AD bioreactors treating a low-strength wastewater. The hypothesis tested was as followed: AD mesophilic sludge has the ability to adapt to low temperature operating conditions through changes in microbial populations' relative abundance and protein expression. To this end, metaproteomics, 16S rRNA gene clone libraries, DGGE fingerprinting and microautoradiography-fluorescence *in*

situ hybridization (MAR-FISH) were applied to comparatively monitor changes in microbial community structure and function during AD bioreactors operated at 37°C and 15°C.

MATERIALS AND METHODS

Bioreactor operation and sample collection. Duplicate expanded granular sludge bed (EGSB) bioreactors (R1 and R2; 3.5 L working volumes) were operated initially at 37°C with a temperature drop to 15°C for comparative analysis after 125 days of operation. Both bioreactors were seeded with an inoculum from a full-scale, internal circulation (IC) reactor operating under mesophilic conditions and used to treat dairy production process wastewaters (Carbery Milk Products, Ireland). In this study, a synthetic low-strength wastewater was used, comprising of volatile fatty acids (VFA; acetic acid, propionic acid, butyric acid) and ethanol with a chemical oxygen demand (COD) ratio of 1:1:1:1. The organic loading rate (OLR) was maintained at 3kg COD m^{-3} d^{-1} with an hydraulic retention time (HRT) of 24 h. This VFA influent represented the later stages of the AD process, providing suitable substrates for acetogenic bacteria and methanogenic archaea. The influent was also supplemented with key minerals (0.3M NH_4Cl, 24 mM $CaCl_2$, 14 mM $MgCl_2$, 3 mM $FeCl_2$, 1.5g l^{-1} yeast extract) and trace elements (0.2 mM $MnCl_2$, 0.2 mM H_3BO_3, 0.1 mM $ZnCl_2$, 0.06 mM $CuCl_2$, 0.01 mM $NaHSO_4$, 0.6 mM $CaCl_2$, 0.07 mM $Nicl_2$, 0.1 mM SeO_2). In addition, a buffering solution (20 mM $NaHCO_3$, 0.5 mM KH_2PO_4, 0.6 mM K_2PHO_4) was added to help maintain neutral pH influent conditions. COD concentrations and % biogas CH4 content were determined according to Standard Methods American Public Health Association (APHA, 1998). Percentage COD removal efficiency was calculated by measuring both influent and effluent COD concentrations. VFA

122 concentrations were determined by using a Varian Saturn 2000 GC/MS system, with
123 CombiPAL autosampler (Varian Inc., Walnut Creek, CA) as previously described
124 (Siggins *et al*., 2011a).
125
126 **Specific methanogenic activity.** Bioreactor biomass from R1 and R2 sampled at
127 37°C (day 125) and 15°C (day 240) were used for specific methanogenic activity
128 (SMA) assays, which were performed in triplicate at both 37°C and 15°C using a
129 pressure transducer technique (Coates *et al*., 1996). Here, acetate (30mM) and H_2/CO_2
130 (80:20, v/v) were employed as substrates in order to measure acetoclastic and
131 hydrogenotrophic activity, respectively. A General Linear Model (GLM) was fitted to
132 the SMA measurements using the statistical package Minitab 16 (www.minitab.com).
133 Assumption of homogeneity of variance was not met however, but by transforming
134 the response variable to the square root SMA, all assumptions of the statistical test
135 were met. The following four attributes were considered: bioreactor (R1 and R2),
136 sludge (day 125 and day 240), substrate (acetate and H_2/CO_2) and assay temperature
137 (37°C and 15°C). Bioreactor was not considered as a factor in the statistical analysis
138 since at each combination of levels of sludge (day 125 and day 240), substrate
139 (acetate and H_2/CO_2) and assay temperature (37°C and 15°C) measurements taken at
140 R1 and R2 were in fact replicates. Furthermore, the two crossed factors sludge and
141 assay temperature were combined into a single factor, named adaptation, at four
142 levels (15AT37, 15AT15, 37AT37 and 37AT15). In addition to examining the main
143 effects of substrate and adaptation, and testing for interaction between these, the GLM
144 analysis included post-hoc analysis to compare each pair of levels of adaptation.
145 The GLM analysis concluded with residual analysis that included graphical
146 diagnostics and rigorous tests to access the assumptions required to justify the

147 statistical inferences. For example, a Kolmogorov-Smirnov test on the residuals gave
148 a P-value>0.15, suggesting no violation of normality of the underlying populations of
149 measurements at the 8 combinations of levels of the factors substrate and adaptation.
150 Furthermore, Levene's test (P-value=0.233) and Bartlett's test (P-value=0.470) gave
151 no evidence of violation of homogeneity of variances of these populations.
152
153 **MAR-FISH.** Microautoradiography (MAR) radiotracer incubations were undertaken
154 at 37°C and 15°C, as outlined by Andreasen and Nielsen (1997) on the same samples
155 that were used for SMA analysis (day 125 and day 240). Briefly, aliquots of 2 ml (c.
156 2-4 g volatile suspended solids [VSS] l^{-1}) sludge granules were incubated immediately
157 after sampling. These incubations were undertaken anaerobically with either acetic
158 acid [1,2-^{14}C] sodium salt or sodium [^{14}C]-bicarbonate (American Radiolabelled
159 Chemicals, Inc.) to target acetoclastic and hydrogenotrophic methanogens,
160 respectively. Twenty μCi (0.74 MBq) of radioactive substrate was added to each
161 sample with [^{14}C]-labelled acetate samples supplemented with unlabelled analogues
162 (2mM final concentration) to ensure radiolabelled substrate was not utilised
163 immediately after adding. In the same context, [^{14}C]-labelled sodium bicarbonate was
164 pressurized with 0.5 bar (95 mV) H_2/CO_2. Each sample (except for incubations with
165 sodium [^{14}C]-bicarbonate) was pressurized with O_2-free N_2 gas. As a control for
166 possible adsorption phenomena, autoclaved sludge granules were also incubated
167 under the same conditions in parallel. Incubations were stopped at different time-
168 points by fixing with paraformaldehyde (PFA final concentration 4% [w/v] in 130
169 mM NaCl and 10 mM Na_3PO_4 [pH 7.2]) for 4 h at 4°C. Samples were washed ten
170 times with 1X PBS to remove excess radioactive substrate and PFA. After embedding
171 granules in OCT freezing medium, serial cryosections of 5-10 μm thickness were

prepared, as previously described (Sekiguchi *et al*., 1999), and immobilized on gelatin coated, acid-washed, coverslips (24 mm x 50 mm; VXR international). Granular sections were then dehydrated and fluorescence *in situ* hybridization (FISH) was performed as described elsewhere (Schramm *et al*., 1998). The Cy3-labelled 16S rRNA targeted probes employed in this study were mixed together for each methanogenic group investigated; i) acetoclastic: *Methanosaeataceae* (Mx825 probe) and *Methanosarcinaceae* (SarcI551 probe) and ii) hydrogenotrophic: *Methanobacteriales* (MB1174 probe) and *Methanomicrobiales* (MG1200b probe) and applied on replicate granular sections throughout the study (Enright *et al*., 2007). The Non388 probe (Wallner *et al*., 1993), complementary to the Eub388 sequence, was used as a negative control. The MAR procedure was undertaken following FISH. First, LM emulsion film (Kodak) was applied to all coverslips, which were then left to expose in complete darkness at 4°C for 4 days. After exposure, coverslips were developed by standard photographic procedures (Andreasen and Nielsen, 1997). An epifluorescent microscope (Carl Zeiss, Oberkochen, Germany) was used for detection of FISH signal, while light microscopy was used to assess silver grain density and MAR-positive cells (cells covered with more than five silver grains; Okabe *et al*., 2005).

DNA and RNA co-extraction. Genomic DNA and total RNA were isolated from granular biomass sampled at 37°C (day 125) and 15°C (days 126, 128, 132 and 240) using a phenol-chloroform-isoamyl alcohol co-extraction method adapted from Carrigg *et al*. (2007). Briefly, 0.5 g of granular biomass for each sample was homogenized (straight after sampling) using a mortar and pestle under liquid nitrogen. Thereafter, 500 µl of 1X CTAB buffer (1% (w/v) CTAB, 0.7 M NaCl, 50 mM Tris-

197 HCl 20 mM EDTA in DEPC-treaded H_2O, pH 8.0) and 500 µl of Phenol:
198 Chloroform: Isoamyl alcohol (25:24:1) was added to each sample along with ~250
199 mg of zirconium beads (125 mg 0.1 mm, 125 mg 0.5 mm). Bead beating (Mini
200 Beadbeater 8; Biospec) was carried out for 30 sec at medium speed (2000 rpm) prior
201 to phase separation by centrifugation at 20000 *g*. Nucleic acids were precipitated from
202 the recovered aqueous phase using PEG (polyethylene glycol) (30% w/v PEG, 1.6M
203 NaCL in DEPC-treated H_2O) for 2 h on ice. The resulting nucleic acids samples were
204 each divided into 2 fractions. One fraction was stored at -20ºC until further use, while
205 the other was immediately processed for DNase treatment followed by cDNA
206 generation (see further below).
207
208 **Clone library construction and sequence analysis.** Amplification of the 16S rRNA
209 gene from DNA extracts (37°C [day 125] and 15°C [day 240]) was achieved using the
210 primer sets 27F (DeLong, 1992) and 1392R (Lane *et al*., 1985) for bacteria and 21F
211 (Lane, 1991) and 958R (DeLong, 1992) for archaea. The PCR cycling conditions
212 were as described in Enright *et al*. (2007). Cloning was carried out using the PCR-
213 XL-TOPO® vector system, with amplified ribosomal DNA restriction analysis
214 (ARDRA) and plasmid sequencing undertaken as outlined by Siggins *et al*. (2012).
215 Any vector contamination was removed by screening sequence data using the
216 National Center for Biotechnology Information (NCBI) Vecscreen software.
217 Sequences were aligned using ClustalX (ClustalX 2.0.12) multiple alignment
218 algorithm with nearest relatives from the BLASTn database and selected sequences
219 downloaded from the Ribosomal Database Project (RDP). Maximum likelihood-based
220 phylogenetic trees were constructed under the GTR + gamma model of DNA
221 substitution implemented RAxML7.0.3 (Stamatakis, 2006) with all parameters

optimised by RAxML. Confidence levels in the phylogeny groupings were assessed using 1000 bootstrap replicates as part of the RAxML phylogeny reconstruction. Diversity indices were calculated using the *vegan* package in MOTHUR (version 1.33.3; Schloss *et al*., 2009). A GLM was performed to compare the diversity indices at 37°C (day 125) and 15°C (day 240) using the statistical package R (www.r-project.org/). Gene sequences recorded in this study were deposited in the GenBank database under the following accession numbers: KC145381-KC145391 (Bacteria; 37°C), KC145392-KC145410 (Bacteria; 15°C), K145412-KC145419 (Archaea; 37°C) and KC182519-KC182527 (Archaea; 15°C).

Quantitative PCR for methanogens. 16S rRNA genes were quantified using a LightCycler 480 instrument (Roche, Mannheim, Germany) and primers and probes from Yu *et al*. (2005) for two acetoclastic families (*Methanosaetaceae* using 702F, 862R and 753P and *Methanosarcinaceae* using 380F, 828R and 492P) and two hydrogenotrophic orders (*Methanomicrobiales* using 282F, 832R and 749P and *Methanobacteriales* using 857F, 1059R and 929P). These methanogenic groups were specifically targeted as they were previously reported to account for the majority of methanogens typically present in anaerobic reactors (Yu *et al*., 2005; Lee *et al*., 2009). DNA extracted at 37°C (day 125) and 15°C (days 128 and 240) was used as template with each reaction mixture prepared as follows: 2 µl PCR-grade water, 1 µl probe (final concentration 200 nM), 1 µl of each primer (final concentration 500 nM), 10 µl of 2x reaction solution and 5 µl of template. All DNA samples were analysed in duplicate, using a two-step thermal cycling protocol consisting of pre-denaturation for 10 min at 94°C, followed by 50 cycles of 10 sec at 94°C and 30 sec at 60°C. Quantitative standard curves were prepared using standard plasmids containing full-

247 length 16S rRNA gene sequences from representative strains of the target
248 methanogenic groups: *Methanosaetaceae* - *Methanosaeta concilli* GP6 (DSM 3671);
249 *Methanosarcinaceae* - *Methanosarcina acetivorans* C2A (DSM 2834),
250 *Methanosarcina barkeri* MS (DSM 800), and *Methanosarcina mazei* Go1 (DSM
251 3647); *Methanomicrobiales* - *Methanospirillum hungatei* JF1 (DSM 864) and
252 *Methanomicrobium mobile* BP (DSM 1539); *Methanobacteriales* -
253 *Methanobacterium formicicum* M.o.H. (DSM 863) and *Methanobrevibacter*
254 *arboriphilicus* DH1 (DSM 1536). The volume-based concentrations (gene copies μl^{-1})
255 were subsequently converted into the biomass-based concentrations (copies per g
256 volatile suspended solid [VSS]) using the VSS concentration of each sludge sample,
257 which was determined gravimetrically.
258
259 **Denaturing gradient gel electrophoresis.** DGGE analysis of archaeal 16S rRNA
260 genes was carried out on both DNA and cDNA extracts (37°C [day 125] and 15°C
261 [days 126, 128, 132 and 240]). Reverse transcription of total RNA was carried out
262 following a method adapted from Corgié *et al*. (2006). Briefly, DNase (Promega)
263 treatment was performed on 5 µl of crude nucleic extracts at 37°C for 30 min. After
264 ensuring that no DNA was present in the RNA samples, by performing control PCRs
265 with DNase treated products, reverse transcription (RT) was carried out using 5 µl of
266 DNase treated templates, 5X first strand buffer, 10 mM of each dNTP, 0.1mM
267 dithiothreitol, 1 U/µl Recombinant Rnasin Ribonuclease Inhibitor, 25 ng/µl random
268 primers and 1 U/µl of SuperScript™ III Reverse Transcriptase (Invitrogen). The RT
269 reaction was performed for 5 min at 25°C, 50 min at 50°C and 15 min at 70°C. PCR
270 amplification of DNA and cDNA was undertaken using primers 787F and 1059R (Yu
271 *et al*., 2005) with a 40-bp GC-clamp attached at the 5'-end of the forward primer to

maintain PCR product stability (Muyzer *et al*., 1993). Touchdown PCR was employed following the protocol described by Janse *et al*. (2004). The resulting PCR products were loaded onto a 10% acrylamide gel containing a 40-65% denaturing gradient (100% denaturant contained 7 M urea and 40% (v/v) formamide) and run at 60°C and 70 V for 16 h in a D-Code system (BioRad, Hercules, CA). Each gel was stained for 30 min with SYBR Gold (30 µl in 300 ml DEPC-treated H_2O) and destained for 15 min. After imaging (UV trans-illumination camera), bands of interest were excised from the gel and eluted in 40 µl of DEPC-treated H_2O. Thereafter, 2 µl of the eluted DNA solution was amplified using the aforementioned primers without the GC clamp. The amplicons were cloned using the TOPO® TA system. After confirming that the cloned sequences were representative of the original band, extracted amplicons were sequenced and the resulting partial 16S rRNA gene sequences were deposited in the GenBank database under the accession numbers: KC305601- KC305623. Phylogenetic analysis was performed using BLASTn and RAxML. Statistical analysis was carried out by creating binary matrices, whereby the presence or absence of bands at different time-points was scored with the numeric values "1" or "0", respectively. The matrix was used to calculate Jaccard's coefficient (a dissimilarity measure) using the xlstat statistical package XLSTAT-2011 software (Addinsoft's http:// www.xlstat.com). The data were then subjected to clustering based on the un-weighted pair group method using arithmetic averages (UPGMA).

Metaproteomics. Proteins were extracted from 50 ml of granular sludge from R1 and R2 sampled at 37°C (day 125) and 15°C (days 128 and 240) with subsequent separation by 2-dimensional gel electrophoresis (2-DGE) using a sonication protocol previously described by Abram *et al*. (2009). Twenty-four gels (four replicates per

297 sampling point per bioreactor) were analyzed using PDQuest-Advanced software,
298 version 8.0.1 (BioRad), with data normalization applied using the local regression
299 model. Protein expression ratios were calculated using average spot intensity
300 (PDQuest) on replicate 2-D gels for each biomass sample taken at 37°C (day 125) and
301 15°C (days 128 and 240). Expression ratios greater than 2.4-fold that were obtained
302 for all replicates were considered significant. Proteins were identified using a
303 combination of tryptic digestion and nanoflow liquid chromatography-electrospray
304 ionization tandem mass spectrometry (nLC-ESI-MS/MS; Abram *et al*., 2011).
305 MS/MS data for +2 to +5 charged precursor ions which exceeded 150 cps were
306 processed using the Paragon™ and ProGroup™ search algorithms (Shilov *et al*.,
307 2007; Guo *et al*., 2007) within ProteinPilot 4.0 software (ABSciex, Foster City, CA)
308 against NCBInr database with no species restriction. Only proteins with ≥ 2 peptides
309 identified at > 99% confidence with a competitor error margin (Prot Score) of 2.00
310 were considered. Pathway repositories such as KEGG (Kanehisa *et al*., 2002) and
311 MetaCyc (Caspi *et al*., 2006) were used to relay functional information on the
312 identified proteins. The Interactive Pathway Explorer iPath2.0 was employed to draw
313 metabolic pathways from which proteins were identified (Yamada *et al*., 2011).
314
315 **RESULTS AND DISCUSSION**
316 **AD bioreactor performance at low temperature is comparable to mesophilic**
317 **operation.** The duplicate bioreactors (R1 and R2) exhibited relatively high
318 performance for the majority of the trial with chemical oxygen demand removal
319 efficiencies (CODRE) consistently above 83% (Table 1; Fig. S1), expect for R2
320 displaying CODRE below 60% after the temperature drop to 15°C (phase period PIV;
321 Table 1). This was most likely due to an observed disruption in the influent

322 recirculation line, which briefly affected the structural integrity of the granular sludge
323 bed in R2. Nevertheless, the percentage methane within the biogas (MB; Table 1) did
324 not appear to be negatively affected and both bioreactors exhibited relatively stable
325 treatment efficiencies for the remainder of the trial, with mean CODRE of >80% and
326 MB of >55% during phase periods PVI and PVII (Table 1; Fig. S1). Immediately
327 after the temperature drop to 15°C (PIV) a sharp increase in effluent acetate
328 concentrations was recorded in both R1 and R2 (Fig. S2), correlating with previous
329 observations (Wu *et al*., 2006; McKeown *et al*., 2009). This increased level of acetate
330 in the bioreactors' effluent was only temporary however, as pre-perturbation
331 concentrations were recorded after ~14 days at 15°C (Fig. S2). Similarly, a slight
332 transient increase in butyric acid effluent concentrations was observed, while the
333 effluent level of propionic acid did not seem to be influenced by the temperature drop
334 (Fig. S2). Taken together, these results suggest that AD microbial communities are
335 resilient to temperature perturbations. Indeed, microbial diversity (Shannon index)
336 increased significantly for both bacteria (P-value=0.016) and archaea (P-value=0.04)
337 from 37°C to 15°C. This was also the case for species richness (Chao1) and evenness
338 (Shannon evenness; Table S1). Overall the performance of AD bioreactors at 15°C
339 was found to be similar to that at 37°C, highlighting the ability of mesophilic granular
340 sludge to adapt to low temperature operation.
341
342 ***Methanomicrobiales*** **abundance increases at low temperature as well as**
343 **hydrogenotrophic methanogenesis.** ARDRA analysis on 384 archaeal clones from
344 R1 and R2 biomass samples collected on day 125 (37°C) and 240 (15°C) led to the
345 identification of 17 unique operational taxonomic units (OTUs; 95.6% recovery rate).
346 Although some OTUs were closely related to the same methanogenic group (e.g.

KC145418 & KC145419), they were still considered as distinct OTUs based on their unique ARDRA profiles. Representative clones from each OTU were sequenced and subsequently assigned to *Euryarchaeota* and *Crenarchaeota* (Fig. 1A). *Methanosarcinales* were found to be predominant in both bioreactors at 37°C and 15°C almost exclusively composed of *Methanosaetacea*-like clones (Fig. 1A; OTUs KC145413 and KC182524 had 98% sequence similarity [Blastn], with 98% sequence similarity to the type strain *M. concilii* GP-6). This was confirmed by qPCR analysis with the detection of over 10^{10} 16S rRNA gene copies per g[VSS]$^{-1}$ from this methanogenic group in all samples analysed (Fig. 2). *Methanosarcinacea* were found to be present in the duplicate reactors throughout the trial but below the quantification limit of the qPCR assay (10^6 copies g[VSS]$^{-1}$; Fig 2). Furthermore, *Methanosarcinaceae* were also detected through cDNA-based DGGE analysis immediately after the temperature drop to 15°C, at days 126, 128 and 132 but not at days 125 (37°C) or 240 (15°C; band 18; Fig. 3A). This suggests that *Methanosarcinaceae* were active members of the microbial community particularly during the period following the temperature drop, which correlated with acetate accumulation in both bioreactors (Fig. S2). The relative abundances of clones assigned to *Crenarchaeota* and *Methanobacteriales* were found to be constant in both bioreactors at 37°C and 15°C (Fig. 1A). *Methanomicrobiales*-like clones were only detected at 15°C for both bioreactors (Fig. 1A), while qPCR highlighted that *Methanomicrobiales* abundance increased at this temperature, particularly towards the end of the trial on day 240 (Fig. 2). Taken together, these observations suggest a more important role for methanogenesis from H_2/CO_2 at low temperature compared to 37°C. This was further supported by SMA and MAR-FISH analyses, which indicated a higher ability of the biomass to produce methane from H_2/CO_2 and a higher

372 incorporation of ^{14}C-bicarbonate at low temperature (day 240 biomass and 15°C
373 assays) when compared to 37°C (day 125 biomass and 37°C assays; Fig. 4; Table 2).
374 Statistical analysis indicated that both substrate (P-value=0.013) and adaptation (P-
375 value<0.005) had a significant effect on SMA measurements, in addition to revealing
376 an interaction effect between these two factors (P-value<0.005). In other words,
377 statistical evidence was found to support that population mean SMA differs at the two
378 levels of substrate and adaptation. Furthermore, pairwise comparisons among the four
379 levels 15AT37, 15AT15, 37AT37 and 37AT15 of adaptation were carried out and
380 highlighted that each two of them had sample means that were significantly different
381 from each other within the GLM model (with all corresponding 6 P-values<0.001;
382 output not shown). While the biomass after 240 days of operation clearly developed
383 the ability to produce methane both from acetate and H_2/CO_2 at 15°C (37AT15 versus
384 15AT15), it also significantly and strikingly increased its ability to do so at 37°C
385 (15AT37 versus 37AT37; Fig. 4). These observations were also reflected in MAR-
386 FISH results (Table 2). It is important to note however, that MAR-FISH only reports
387 on labeled substrates incorporation into biomass, and this does not necessarily involve
388 a catabolic reaction. Hydrogenotrophic methanogens can assimilate acetate via acetyl
389 CoA with subsequent reductive carboxylation to pyruvate (Oberlies *et al*., 1980). The
390 finding that no MAR-positive cells were recorded for hydrogenotrophic methanogens
391 when incubated with [^{14}C]-labelled acetate may indicate that acetoclastic
392 methanogens and homacetogenic bacteria outcompeted this group at both operating
393 temperatures for this substrate (Table 2).
394
395 DGGE analysis of the archaeal community highlighted that DNA and cDNA patterns
396 differed with the identification of two corresponding clusters throughout the trial for

both bioreactors (Fig. 3C). The detection of microorganisms assigned to *Crenarchaeota* (band 7 and 13, Fig. 3), *Methanobacteriales* (band 5 and 15, Fig. 3), *Methanosarcinales* (band 6 and 18, Fig. 3) and *Methanomicrobiales* (band 4, 16, 17 and 22, Fig. 3) in cDNA samples suggests that these represented active members of the AD microbiome at the time of sampling. Taken together the archaeal community was found to be very similar in both bioreactors and largely stable throughout the trial with an increased role for hydrogenotrophic methanogenesis at lower temperature.

Bacterial clone libraries (comprising of 365 clones) recorded 6 phyla with 30 unique OTUs (91.8% recovery rate). *Proteobacteria*-like clones were found to be predominant in both bioreactors at 37°C and 15°C, with a relative abundance ranging from 48% (R1 at 37°C) to 62% (R2 at 37 and 15°C; Fig. 1B). This observation was in agreement with previous findings (Siggins *et al*., 2011b). For the two bioreactors at 37ºC, *Proteobacteria* were mainly composed of *Desulfuromonas*-like clones with only two OTUs recorded. At the end of the trial, a higher number of OTUs were assigned to *Proteobacteria* with *Syntrophaceae*-like clones accounting for over 10% of the bacterial clone library on day 240 at 15ºC (Fig. 1B). The relative abundance of other bacterial groups was also impacted by the operating temperature; for example, a decrease in clones assigned to *Firmicutes* was observed at 15°C when compared to 37°C (from 14% to 9% for R1 and 12% to 1% for R2; Fig. 1B). Also, for R2, there was an increase in *Synergistetes*-like clones at low temperature, represented by a single OTU comprising 14% of bacterial clone library in this sample. In addition, *Tenericutes*-like clones were identified at 15°C for R2, while this group was not represented in this bioreactor at 37°C or in R1. Overall, phylogenetic analyses highlighted similar trends in the duplicate bioreactors throughout the trials with

422 relatively stable archaeal and bacterial communities. *Methanosarcinales* and
423 *Proteobacteria* were found to be predominant at 37°C and 15ºC, with an increase of
424 *Methanomicrobiales* and a decrease of *Firmicutes* recorded at low temperature.
425
426 **Adaptation to psychrophilic AD encompasses increased protein expression.** The
427 high level of COD removal after the temperature drop suggests that the mesophilic
428 sludge adapted quickly to 15ºC through discrete changes in microbial community
429 function (Fig. S1). In order to assess this further, metaproteomics was carried out.
430 The prevalence of *Methanosarcinales* and *Proteobacteria* highlighted by
431 phylogenetic analysis was supported by metaproteomics. A total of 77 microbial
432 proteins expressed at 37ºC (day 125) and at 15ºC (day 128 and day 240) were
433 identified, amongst which, 39 (51%) were assigned to *Methanosaetaceae* and 21
434 (27%) to *Proteobacteria* (Table 3; Table S2; Fig. S3). For protein identification and
435 assignment, four situations arose: i) one 2D-gel spot led to the identification of one
436 protein assigned to a specific microbial group *via* the identification of one set of
437 peptides (e.g. spot C1 - phosphate binding protein from *Methanosaeta concilii*; Table
438 S2); ii) one protein assigned to a specific microbial group migrated to different spots
439 on the gels (e.g. acetyl-CoA synthetase from *Methanosaeta concilii*; Table S2); iii)
440 one gel spot led to the identification of different peptide sets from several proteins
441 assigned to different microbial groups with a common or different function (e.g. spot
442 B1 or spot B11; Table S2); and iv) one gel spot led to the identification of one peptide
443 set from one protein assigned to different microbial groups, in this case the lowest
444 common ancestor was selected for microbial assignment (e.g. spot B28 - iron-
445 containing alcohol dehydrogenase from *Pseudomonaceae*; Table S2). Amongst the 62
446 gel spots that returned positive hits for protein identification, only 10 (~16%) were

447 associated with a single protein, making the interpretation of differential expression
448 somewhat difficult (Table S2). Indeed, for example, in the case of spot B1, from
449 which 2 different sets of peptides were identified, each assigned to acetyl-CoA
450 synthetases from *M. concilii* and *Syntrophus aciditrophicus*, it is not possible to
451 distinguish which protein (or both) is responsible for the increased spot intensity at
452 day 240 (15ºC) compared to day 128 (15ºC, straight after the temperature drop; Table
453 S2). Some trends, however, could be observed regarding differential protein
454 expression under the diverse operating conditions. Overall, amongst the spots for
455 which clear protein ratio trends could be reported, 16 were found to correspond to
456 proteins with increased expression at 15°C (day 240), against only 5 showing higher
457 signal intensity at 37°C and 12 with no apparent differential expression between the 2
458 temperatures (Table S2). This could possibly be indicative of increased microbial
459 activity at 15°C when compared to 37°C, which is also supported by SMA and MAR-
460 FISH analyses (Fig. 4; Table 2).
461
462 An overview of the metabolic pathways in which proteins were detected is shown in
463 Figure S4. Evidence of acetate, ethanol, propionate and butyrate degradation could be
464 obtained, as well as methanogenesis from acetate and from CO_2 under all the
465 operating conditions investigated (day 125, 128 and 240; Table 3). Specifically,
466 proteobacterial groups were responsible for ethanol degradation through the
467 expression of iron containing alcohol dehydrogenase (Fe-ADH). These included
468 *Geobacteraceae* (δ -Proteobacteria), who have been previously shown to engage in
469 syntrophic relationships with acetoclastic methanogens through direct interspecies
470 electron transfer (DIET) (Morita *et al*., 2011; Rotaru *et al*., 2014). The bioconversion
471 of propionate and butyrate was also evident with metabolic proteins associated with

472 the degradation of these VFAs positively identified for bacterial groups (e.g. Butyryl-
473 CoA dehydrogenase, *Thermodesulfobacterium* sp.; Table 3). Enzymes from
474 glycolysis/gluconeogenesis, pentose phosphate pathway, TCA cycle and amino acid
475 biosynthesis were also detected. The identification of acetyl-CoA synthase assigned to
476 *Methanosaetaceae* (Table 3) together with the relatively low acetate concentrations
477 recorded throughout the majority of the trial (Fig. S2) suggests that this group was
478 responsible for driving acetate oxidation in both bioreactors. The efficiency of
479 acetoclastic methanogenesis at 15ºC was also confirmed by SMA and MAR-FISH
480 (Fig. 4; Table 2), with both methods showing that biomass from day 240 had a higher
481 level of substrate uptake (for acetate and H_2/CO_2) when compared to biomass
482 sampled on day 125. It is important to note that although H_2CO_2 was not added to
483 SMA vials testing for acetoclastic methanogenesis, acetate could also have been
484 converted to H_2CO_2 by homoacetogenic bacteria (such as *Dethiobacter* sp. identified
485 in proteomic data) with subsequent utilization by hydrogenotrophic methanogens.
486 This may have been especially important during low temperature incubations. A
487 coenzyme F_{420} hydrogenase assigned to *M. concilii* was detected throughout the trial
488 and was found to be expressed at higher level on day 240 (15ºC) compared to day 125
489 (37ºC) and day 128 (15ºC; Table S2). This enzyme is usually associated with
490 methylotrophic methanogenesis, which requires a reduced coenzyme F_{420} (F_{420}, H_2;
491 Hendrickson & Leigh, 2008). ^{14}C-bicarbonate uptake from acetoclastic methanogens
492 was also reported from biomass sampled at both 37ºC (day 125) and 15ºC (day 240)
493 possibly indicating the ability of these archaeal populations to produce methane from
494 CO_2 (Rotaru *et al*., 2014; Gunnigle *et al*., 2015). Zhu and colleagues (2012) proposed
495 that *Methanosaeta spp*. can use the methyl group oxidation pathway as a shunt during
496 acetoclastic metabolism, which could generate reducing equivalents for biomass

497 synthesis. It is also worth noting that the genus status of *Methanosaeta* is currently
498 under discussion (Tindall, 2014). Coenzyme F_{420} hydrogenase can also function in a
499 membrane-bound ferredoxin:heterodisulfide oxidoreductase system, generating an
500 electrochemical gradient driving ATP synthesis (Welte and Deppenmeier, 2011),
501 which might be relevant for *Methanosaeta* since they lack genes encoding for energy
502 conserving hydrogenase (Ech; Zhu *et al*., 2012). As *Methanosaetaceae* rely on an
503 energy costly system for the activation of acetate requiring the hydrolysis of two ATP
504 molecules (Smith and Ingrim-Smith, 2007), the increased expression of this enzyme
505 at low temperature could possibly be an energy conservation strategy. Of particular
506 note was the increased expression of a bifunctional formaldehyde activating
507 enzyme/3-hexulose-6-phosphate synthase protein (Fae/HPS) assigned to *M*. *concilii* at
508 the end of the trial (Table S2). This enzyme, which contains 2 active domains, has the
509 ability to catalyze two reactions involving formaldehyde as a substrate (Grochowski
510 *et al*., 2005). While Fae can combine formaldehyde and tetrahydromethanopterin to
511 produce 5,10-methylene-tetrahydromethanopterin (an intermediate of methanogenesis
512 from CO_2), HPS can drive the conversion of formaldehyde and D-ribulose-5-
513 phosphate (an intermediate of the pentose phosphate pathway) to hexulose-6-
514 phosphate, which can be further converted to D-fructose-6-phosphate (a glycolytic
515 intermediate). The same observation was reported in different sets of reactors with an
516 increased expression of Fae/HPS as the operating temperature decreased (from 37ºC
517 to 15ºC and then to 7ºC; Gunnigle *et al*., 2015). Finally, proteins from major
518 chaperone families including DnaK and GroEL were expressed at higher levels at
519 lower temperatures (Table S2), indicating that even after a prolonged period of
520 operation at 15ºC mesophilic microbial communities were still experiencing some

level of stress (Rince *et al*., 2000; Muga and Moro, 2008; Sala *et al*., 2014; Singh and Jiang, 2015).

Many other methanogenic groups displayed functional dynamics during this bioreactor trial as indicated by both cDNA-based DGGE and metaproteomics (Fig. 3; Table S2). Interestingly, archaeal diversity was recorded at a much higher level in cDNA-based DGGE profiles compared to DNA-based profiles, with cluster analysis highlighting this divergence (Fig. 3C). Specific methanogenic groups detected in cDNA bands included the hydrogen-utilizing *Methanolinea* and *Methanospirillacea*e, in the order *Methanomicrobiales* (Fig. 3A). The metabolic significance of *Methanomicrobiales* during the trial was confirmed through the identification of eight (15% of archaeal) proteins assigned to this group that were expressed at higher level at 15ºC (Table S2). The majority of these proteins were assigned to *Methanospirillacea*e, known to scavenge hydrogen during low temperature AD operation (Tsushima *et al*., 2010). *Methanospirillaceae* can form syntrophic relationships with fermenting bacteria such as *Syntrophus sp*. (de Bok *et al*., 2005; Schmidt *et al*., 2013) and multiple proteins assigned to syntrophic bacteria were somewhat expressed at a higher level in low temperature biomass (Table S2). Overall, metaproteomics together with SMA and MAR-FISH analyses indicated an increased microbial activity from AD bioreactor biomass adapted to 15ºC compared to the initial mesophilic biomass from the same bioreactors operated at 37ºC. Interestingly, however, AD bioreactor performance at 15ºC was reported to match and not to outperform that of mesophilic operation. This could be possibly attributed to the lower mass transfer occurring at lower temperature when compared to 37ºC, which could lead to the necessity of producing more proteins to convert the same amount of

546 substrate per unit of time. The increased methanogenic activity reported at 37ºC from
547 the 15ºC biomass (day 240) compared to the 37ºC biomass (day 125; 15AT37 versus
548 37AT37; Fig. 4) could potentially be a transient result from the increased *in situ*
549 protein expression at the time of sampling. The change in SMA assay temperature
550 from 15ºC to 37ºC for the biomass sampled on day 240 (15AT15 versus 15AT37; Fig.
551 4) resulted in elevated CH_4 production from acetate but not from H_2/CO_2. This could
552 be partly due to a lower level of substrate availability at 37ºC compared to 15ºC as
553 CO_2 solubility decreases with increasing temperature. This, in turn could have an
554 effect on acetoclastic methanogens by reducing substrate competition at 37ºC. Indeed,
555 MAR-FISH indicated that these methanogenic populations had the ability to take up
556 ^{14}C bicarbonate at the two temperatures investigated. However, this uptake was
557 observed to occur after 5 minutes of incubation at 15ºC, against 10 minutes at 37ºC
558 for biomass sampled at day 240 (15ºC), while the reverse trend was observed for
559 acetate (Table 2). Finally the ability to take up ^{14}C bicarbonate from hydrogenotrophic
560 populations was not impacted by the change in SMA assay temperature for the same
561 biomass (day 240 at 15ºC; Fig. 4). Taken together, these results suggest a higher
562 contribution of hydrogenotrophic methanogenesis during bioreactor operation at 15ºC
563 than at 37ºC, which could be partly attributed to an increase in abundance of
564 hydrogenotrophic methanogens but could also involve substrate competition for
565 acetoclastic populations.
566
567 **Conclusions**
568 This study integrated metaproteomics with genomic (DNA and RNA) and
569 physiological data recovered from samples taken over the course of a psychrophilic
570 AD bioreactor trial, from which the following conclusions could be inferred:

571

572 (1) DNA-based phylogenetic data were consistent with metaproteomic profiles for
573 characterising the most predominant microbial groups throughout the bioreactor trial.
574 (*Methanosaetaceae* and *Proteobacteria*).

575

576 (2) RNA-derived DGGE analysis uncovered metabolically active groups that the
577 DNA-based comparative approach missed e.g. transient occurrence of
578 *Methanosarcinaceae* directly after the temperature drop event where acetate
579 accumulation was recorded.

580

581 (3) *Methanosaetaceae* were found to drive acetoclastic methanogenesis at both
582 operation temperatures, with possible energy conservation through a coenzyme F_{420}
583 hydrogenase driven system. In addition, acetoclastic methanogens were also reported
584 to take up ^{14}C-bicarbonate.

585

586 (4) SMA and MAR-FISH were consistent in highlighting the increase of
587 hydrogenotrophic methanogens in 15°C biomass, as characterised by genomic and
588 metaproteomic results.

589

590 (5) Changes in microbial community structure (phylogenetic diversity) and function
591 (protein expression) were found to underpin the adaptation of mesophilic sludge to
592 LtAD.

593

594 Finally, future molecular experiments applied to psychrophilic AD would benefit
595 greatly from integrating metagenomes derived from the AD environment. This would

facilitate high-impact proteomic resolution, which could in turn support the discovery of novel genes and proteins for bio-industrial applications.

Funding

This work was supported by Science Foundation Ireland (Grants RFP 08/RFP/EOB1343 and 06/CP/E006) and the Wellcome Trust (grant number GR06281AIA), which funded the purchase of the QStar XL mass spectrometer at the BSRC Mass Spectrometry and Proteomics Facility, University of St Andrews.

Acknowledgements

The authors would like to thank Camilla Thorn and Gustavo Sambrano for useful discussions.

REFERENCES

Abram F. Systems-based approaches to unravel multi-species microbial community functioning. *Comput Struct Biotechnol J* 2015;**13**:24-32.

Abram F, Gunnigle E, O'Flaherty V. Optimisation of protein extraction and 2-DE for metaproteomics of microbial communities from anaerobic wastewater treatment biofilms. *Electrophoresis* 2009;**30**:4149-51.

Abram F, Enright AM, O'Reilly J *et al*. A metaproteomic approach gives functional insights into anaerobic digestion. *J Appl Microbiol* 2011;**110**:1550-60.

Andreasen K, Nielsen PH. Application of microautoradiography to the study of substrate uptake by filamentous microorganisms in activated sludge. *Appl Environ Microbiol* 1997;**63**;3662–68.

APHA. (1998) Standard methods for the examination of water and wastewater In: Clesceri, L.S., Greenberg, A.E., Eaton, A.D (Eds.), Washington, DC, U.S.A.

Bailey VL, Fansler SJ, Stegen JC, *et al*. Linking microbial community structure to beta-glucosidic function in soil aggregates. *ISME J* 2013;**7**:2044-53.

de Bok FAM, Stams AJM, Dijkema C *et al*. Pathway of propionate oxidation by a syntrophic culture of *Smithella propionica* and *Methanospirillum hungatei*. *Appl Environ Microbiol* 2001;**67**:1800-4.

de Bok FAM, Harmsen HJ, Plugge CM *et al*. The first true obligately syntrophic propionate-oxidizing bacterium, *Pelotomaculum schinkii* sp. nov., co-cultured with *Methanospirillum hungatei*, and emended description of the genus *Pelotomaculum*. *Int J Syst Evol Microbiol* 2005;**55**:1697-703.

Burke C, Steinberg P, Rusch D *et al*. Bacterial community assembly based on functional genes rather than species. *Proc Natl Acad Sci USA* 2011;**108**:14288-93.

632 Carrigg C, Rice O, Kavanagh S *et al*. DNA extraction method affects microbial
633 community profiles from soils and sediment. *App Microbiol Biotechnol* 2007;**77**:955-
634 64.
635 Caspi R, Foerster H, Fulcher CA *et al*. MetaCyc: a multiorganism database of
636 metabolic pathways and enzymes. *Nucl Acid Res* 2006;**34**:511-6.
637 Coates JD, Coughlan MF, Colleran E. Simple method for the measurement of the
638 hydrogenotrophic methanogenic activity of anaerobic sludge's. *J Microbiol Meth*
639 1996;**26**:237-46.
640 Collins G, Foy C, McHugh S *et al*. Anaerobic biological treatment of phenolic
641 wastewater at 15-18°C. *Water Res* 2005;**39**:1614-20.
642 Corgié SC, Beguiristain T, Leyval C. Profiling 16S bacterial DNA and RNA:
643 Difference between community structure and transcriptional activity in phenanthrene
644 polluted sand in the vicinity of plant roots. *Soil Biol Biochem* 2006;**38**:1545-53.
645 DeLong EF. Archaea in coastal marine sediments. *Proc Natl Acad Sci USA*
646 1992;**89**:5685-9.
647 Enright AM, Collins G, O'Flaherty V. Temporal microbial diversity changes in
648 solvent-degrading anaerobic granular sludge from low-temperature (15°C) wastewater
649 treatment bioreactors. *Sys App Microbiol* 2007;**30**:471-82.
650 Grochowski L, Xu H and White RH. Ribose-5-phosphate biosynthesis in
651 *Methanocaldococcus jannaschii* occurs in the absence of a pentose-phosphate
652 pathway. *J Bacteriol* 2005;**187**:7382-9.
653 Gunnigle E, Siggins A, Botting CH *et al*. Low-temperature anaerobic digestion is
654 associated with differential methanogenic protein expression. *FEMS Microbiol Lett*
655 2015;**362**:fnv059.

656 Guo T, Wang W, Rudnick PA *et al*. Proteome analysis of microdissected formalin-
657 fixed and paraffin-embedded tissue specimens. *J Histochem Cytochem* 2007;**55**:763-
658 72.
659 Hendrickson EL, Leigh JA. Roles of coenzyme F_{420}-reducing hydrogenases and
660 hydrogen- and F_{420}-dependent methylenetetrahydromethanopterin dehydrogenases in
661 reduction of F_{420} and production of hydrogen during methanogenesis. *J Bacteriol*
662 2008;**190**:4818-21.
663 Janse I, Bok J, Zwart G. A simple remedy against artifactual double bands in
664 denaturing gradient gel electrophoresis. *J Microbiol Meth* 2004;**57**:279-81.
665 Jansson JK, Neufeld JD, Moran MA *et al*. Omics for understanding microbial
666 functional dynamics. *Environ Microbiol* 2012;**14**:1-3.
667 Kanehisa M, Goto S, Kawashima S *et al*. The KEGG databases at GenomeNet. *Nucl*
668 *Acid Res* 2002;**30**:42-46.
669 Lane DJ, Pace B, Olsen GJ *et al*. Rapid determination of 16S ribosomal RNA
670 sequences for phylogenetic analysis. *Proc Natl Acad Sci USA* 1985;**82**:6955-9.
671 Lane DJ. 16S/23S rRNA sequencing. In: Stackebrandt E, Goodfellow M (ed.).
672 *Nucleic acid techniques in bacterial systematics*. Chichester, England: John Wiley &
673 Sons, 1991,115-75.
674 Lee C, Kim J, Hwang K *et al*. Quantitative analysis of methanogenic community
675 dynamics in three anaerobic batch digesters treating different wastewaters. *Water Res*
676 2009;**43**:157-165.
677 McKeown R, Scully C, Enright AM *et al*. Psychrophilic methanogenic community
678 development during long-term cultivation of anaerobic granular biofilms. *ISME J*
679 2009;**3**:1231-42.

McKeown R, Hughes D, Collins G *et al*. Low-temperature anaerobic digestion for wastewater treatment. *Biotechnol* 2012;**23**:444-51.

Morita M, Malvankar NS, Franks AE *et al*. Potential for Direct Interspecies Electron Transfer in Methanogenic Wastewater Digester Aggregates. *mBio* 2011; **2**:e00159-11.

Muga A, Moro F. Thermal adaptation of heat shock proteins. *Curr Protein Pept Sci* 2008;**9**:552-66.

Muller EEL, Glaab E, May P *et al*. Condensing the omics fog of microbial communities. *Trends Microbiol* 2013;**21**:325-33.

Muyzer G, de Waal EC, Uitterlinden AG 1993. Profiling of complex microbial populations by denaturing gradient gel electrophoresis analysis of polymerase chain reaction-amplified genes coding for 16S ribosomal RNA. *Appl Environ Microbiol* 1993;**59**:695-700.

Nielsen PH, Nielsen JL. Microautoradiography: recent advances within the studies of the ecophysiology of bacteria in biofilms. *Water Sci Technol* 2005;**52**:187-94.

Nikolausz M, Palatinszky M, Rusznyak A *et al*. Novel approach using substrate-mediated radiolabelling of RNA to link metabolic function with the structure of microbial communities. *FEMS Microbiol Lett* 2007;**274**:154-61.

Oberlies G, Fuchs, G, Thauer RK. Acetate Thiokinase and the assimilation of acetate in Methanobacterium thermautotrophicum. *Arch Microbiol* 1980;**128**:24-52.

Okabe S, Kindaichi T, Ito T. Fate of ^{14}C-labelled microbial products derived from nitrifying bacteria in autotrophic nitrifying biofilms. *Appl Environ Microbiol* 2005;**71**:3987–94.

Ramirez I, Volcke EIP, Rajinikanth R *et al*. Modeling microbial diversity in anaerobic digestion through an extended ADM1 model. *Water Res* 2009;**43**:2787-800.

Rince A, Flahaut S, Auffray Y. Identification of general stress genes in *Enterococcus faecalis*. *Int J Food Microbiol* 2000;**55**:87-91.

Rotaru AE, Shrestha PM, Liu F *et al*. A new model for electron flow during anaerobic digestion: direct interspecies electron transfer to *Methanosaeta* for the reduction of carbon dioxide to methane. *Energy Environ Sci* 2014;**7**:408-15.

Sala A, Bordes P, Genevaux P. Multitasking SecB chaperones in bacteria. *Front Microbiol* 2014;**5**:666.

Schloss PD, Westcott SL, Ryabin T *et al*. Introducing mothur: open-source, platform-independent, community-supported software for describing and comparing microbial communities. *Appl Environ Microbiol* 2009; **75**:7537-7537.

Schmidt A, Müller N, Schink B *et al*. A proteomic view at the biochemistry of syntrophic butyrate oxidation in *Syntrophomonas wolfei*. *Plos One* 2013;**8**:e56905.

Schramm A, de Beer D, Wagner M *et al*. Identification and activity *in situ* of *Nitrosospira* and *Nitrospira* spp. as dominant populations in a nitrifying fluidized bed reactor. *Appl Environ Microbiol* 1998;**64**:3480-5.

Sekiguchi Y, Kamagata Y, Nakamura K *et al*. Fluorescence in situ hybridization using 16S rRNA- targeted oligonucleotides reveals localization of methanogens and selected uncultured bacteria in mesophilic and thermophilic sludge granules. *Appl Environ Microbiol* 1999;**65**:1280-8.

Shilov IV, Seymour SL, Patel AA *et al*. The Paragon algorithm, a next generation search engine that uses sequence temperature values and feature probabilities to identify peptides from tandem mass spectra. *Mol Cell Proteom* 2007;**6**:1638-55.

Siggins A, Enright AM, O'Flaherty V. Low-temperature (7°C) anaerobic treatment of a trichloroethylene-contaminated wastewater: Microbial community development. *Water Res* 2011a;**45**:4035-46.

729 Siggins A, Enright AM and O'Flaherty V. Temperature dependent (37°C-15°C)
730 anaerobic digestion of a trichloroethylene-contaminated wastewater. *Bioresource*
731 *Technol* 2011b;**102**(17):7645-56.
732 Siggins A, Enright AM, Abram F *et al*. Impact of Trichloroethylene Exposure on the
733 Microbial Diversity and Protein Expression in Anaerobic Granular Biomass at 37°C
734 and 15°C. *Archaea* 2012;doi:10.1155/2012/940159.
735 Singh R, Jiang X. Expression of stress and virulence genes in *Escherichia coli*
736 O157:H7 heat shocked in fresh dairy compost. *J Food Prot* 2015;**78**:31-41.
737 Smith KS, Ingram-Smith C. *Methanosaeta*, the forgotten methanogen? *Trends*
738 *Microbiol* 2007;**15**:150-5.
739 Stamatakis A. RAxML-VI-HPC: maximum likelihood-based phylogenetic analyses
740 with thousands of taxa and mixed models. *Bioinformatics* 2006;**22**:2688-90.
741 Tindall BJ. The genus name *Methanothrix* Huser *et al*. 1983 and the species
742 combination *Methanothrix soehngenii* Huser *et al*. 1983 do not contravene Rule 31a
743 and are not to be considered as rejected names, the genus name *Methanosaeta* Patel
744 and Sprott 1990 refers to the same taxon as *Methanothrix soehngenii* Huser *et al*.
745 1983 and the species combination *Methanothrix thermophila* Kamagata *et al*. 1992 is
746 rejected: Supplementary information to Opinion 75. Judicial Commission of the
747 International Committee on Systematics of Prokaryotes. *Int J Syst Evol Microbiol*
748 2014;**64**(Pt 10):3597-8.
749 Thauer RK, Kaster AK, Seedorf H et al. Methanogenic archaea: ecologically relevant
750 differences in energy conservation. *Nat Rev Microbiol* 2008;**6**:579-91.
751 Tsushima I, Yoochatchaval W, Yoshida H *et al*. Microbial community structure and
752 population dynamics of granules developed in expanded granular sludge bed (EGSB)

reactors for the anaerobic treatment of low-strength wastewater at low temperature. *J Environ Sci* 2010;**45**:754-66.

Wallner G, Amann R, Beisker W. Optimising fluorescent in situ hybridization of suspended cells with rRNA-targeted oligonucleotide probes for the flow cytometric identification of microorganisms. *Cytometry* 1993;**14**:136-43.

Welte C, Deppenmeier U. Membrane-bound electron transport in *Methanosaeta thermophila*. *J Bacteriol* 2011;**193**:2868-70.

Wu MC, Sun KW, Zhang Y. Influence of temperature fluctuation on thermophilic anaerobic digestion of municipal organic solid waste. *J Zhejiang Univ Sci B* 2006;**7**:180-5.

Yamada T, Letunic I, Okuda S *et al*. iPath2.0: interactive pathway explorer. *Nucleic Acids Res* 2011;**39**:W412-15.

Yu Y, Lee C, Kim J *et al*. Group-specific primer and probe sets to detect methanogenic communities using quantitative real-time polymerase chain reaction. *Biotechnol*. *Bioeng* 2005;**89**:670-9.

Zhang D, Zhu W, Tang C, *et al*. Bioreactor performance and methanogenic population dynamics in a low-temperature (5-18°C) anaerobic fixed-bed reactor. *Biores Technol* 2012;**104**:136-43.

Zhi W, Ge Z, He Z, *et al*. Methods for understanding microbial community structures and functions in microbial fuel cells: A review. *Biores Technol* 2014;**171**:461-8.

Zhu J, Zheng H, Ai G, *et al*. The genome characteristics and predicted function of methyl-group oxidation pathway in the obligate aceticlastic methanogens, *Methanosaeta* spp. *PloS One* 2012;**7**(5):e36756.

Table 1 Summary of R1 and R2 operational performance during trial

		37°C			15°C			
Phase period		**PI**	**PII**	**PIII**	**PIV**	**PV**	**PVI**	**PVII**
Days		0-40	41-80	81-125	126-132	133-160	161-200	200-240
CODRE[a]								
	R1	91(3)	90(5)	96(2)	86(5)	88(6)	88(4)	92(2)
	R2	90(7)	88(6)	91(4)	54(22)	68(8)	83(6)	88(7)
MB[b]								
	R1	66(9)	60(7)	58(9)	62(12)	64(8)	61(4)	56(9)
	R2	63(6)	51(11)	57(7)	61(16)	63(6)	58(11)	57(9)
MY[c]								
	R1	5.67(0.56)	6.74(0.56)	8.23(1.02)	5.24(0.69)	6.39(0.87)	7.56(1.01)	8.03(0.78)
	R2	5.72(0.61)	6.22(0.74)	7.56(0.72)	4.23(1.42)	6.42(0.78)	7.23(0.73)	7.61(0.92)

[a]Chemical oxygen demand removal efficiency (%), where values are the period mean (standard deviation in parentheses)
[b]Methane (CH_4) in biogas (%), where values are the period mean (standard deviation in parentheses)
[c]Methane (CH_4) yield (L), where values are the period mean with measurements taken on a weekly basis (standard deviation in parentheses)

Table 2: Relative abundance of MAR-positive cells following uptake of ^{14}C-labelled substrates in coordination with archaeal hybridisation probes at 37°C and at 15°C.

Trial day (operating temperature)	**125** (37°C)				**240** (15°C)				**125** (37°C)				**240** (15°C)			
MAR Substrate[a]	**^{14}C Acetic Acid**								**H_2, Sodium ^{14}C Bicarbonate 37°C**							
Assay Temperature	**37°C**								**37°C**							
Incubation time (hours)	5	10	15	20	5	10	15	20	5	10	15	20	5	10	15	20
Acetoclastic probe mix[b]																
Mx825 + SarcI551 (R1)	++	+++	+++	+++	+++	+++	+++	+++	-	+	+	++	-	++	++	++
Mx825 + SarcI551 (R2)	++	+++	+++	+++	+++	+++	+++	+++	-	+	++	++	-	+	++	++
Hydrogenotrophic probe mix																
MB1174 + MG1200b (R1)	-	-	-	-	-	-	-	-	+	++	++	+++	++	+++	+++	+++
MB1174 + MG1200b (R2)	-	-	-	-	-	-	-	-	+	++	++	+++	++	+++	+++	+++
Assay Temperature	**15°C**								**15°C**							
Incubation time (hours)	5	15	25	35	5	15	25	35	5	15	25	35	5	15	25	35
Acetoclastic probe mix																
Mx825 + SarcI551 (R1)	+	+	++	+++	++	+++	+++	+++	-	-	+	++	+	+	++	++
Mx825 + SarcI551 (R2)	+	+	++	+++	++	+++	+++	+++	-	-	+	++	+	++	++	++
Hydrogenotrophic probe mix																
MB1174 + MG1200b (R1)	-	-	-	-	-	-	-	-	-	+	++	++	++	+++	+++	+++
MB1174 + MG1200b (R2)	-	-	-	-	-	-	-	-	-	+	++	++	++	+++	+++	+++

[a]R1: bioreactor 1; R2: bioreactor 2
[b]- No uptake of substrate recorded; + < 10% of the total MAR-positive cells; ++ 10-50% of the MAR-positive cells; +++ > 50% of the MAR-positive cells

790 **Table 3** Identification and putative function of proteins excised from 2-D gels from
791 anaerobic granular biomass of reactors R1 and R2 at 37°C (day 125) and at 15°C (day
792 128 and day 240).

Protein name	Accession number(s)	Microbial assignment	Suggested Function
General metabolism & biosynthesis			
Acetyl-coA synthetase	gi|330506786	*Methanosaeta concilii*	Acetate utilisation
Acetyl-coA synthetase	gi|499737809	*Syntrophus aciditrophicus*	Acetate utilisation
Glutaconate-CoA transferase	gi|495794133	*Dethiobacter alkaliphilus*	Acetate formation
Butyryl-CoA dehydrogenase	gi|334902573	*Thermodesulfobacterium sp.*	Butyrate degradation
Iron-containing alcohol dehydrogenase	gi|500472455 gi|500471288 gi|501811427	*Geobacter sp.*	Ethanol degradation
Iron-containing alcohol dehydrogenase	gi|505938069	*Desulfobulbus propionicus*	Ethanol degradation
Iron-containing alcohol dehydrogenase	gi|499652122 gi|330981490 gi|330957848	*Pseudomonaceae*	Ethanol degradation
Enolase	gi|330506450	*M. concilii*	Glycolysis/ Gluconeogenesis
Triose-P isomerase	gi|330508946	*M. concilii*	Glycolysis/ Gluconeogenesis
Fructose-biP aldolase	gi|88602327	*Methanospirillium hungatei*	Glycolysis/ Gluconeogenesis
PfkB domain protein	gi|330507700	*M. concilii*	Pentose phosphate pathway
3-hexulose-6-P synthase	gi|330506676	*M. concilii*	Formaldehyde assimilation
Bifunctional formaldehyde activating enzyme/3-hexulose-6-P synthase	gi|330507450	*M. concilii*	Formaldehyde assimilation
Succinyl-CoA synthetase β-subunit	gi|500017842	*S. fumaroxidans*	TCA cycle
Bifunctional short chain isoprenyl diP synthase	gi|330508369	*M. concilii*	Biosynthesis of secondary metabolites
Aminotransferase	gi|330508265	*M. concilii*	Lysine biosynthesis
Dihydrodipicolinate synthase	gi|330506987	*M. concilii*	Lysine biosynthesis
Dihydroxy-acid dehydratase	gi|330507263	*M. concilii*	Amino acid biosynthesis
Ketol-acid reductoisomerase	gi|330506661	*M. concilii*	Amino acid biosynthesis
Ketol-acid reductoisomerase	gi|88602531	*M. hungatei*	Amino acid biosynthesis
Phosphoribosylformyl-glycinamidine synthase II	gi|330506496	*M. concilii*	Purine metabolism
Adenylylsulfate reductase α-subunit	gi|151302335 gi|151302332 gi|18034269	*Syntrophobacteraceae*	Sulfur metabolism
Adenylylsulfate reductase α-subunit	gi|500017195	*S. fumaroxidans*	Sulfur metabolism
Dissimilatory sulphite reductase α-subunit	gi|505941299	*D. propionicus*	Sulfur metabolism
Hydroxylamine reductase	gi|330507988	*M. concilii*	Nitrogen metabolism
Aldehyde oxidoreductase	gi|505938067	*D. propionicus*	Oxidation reduction
Sulfate adenylyltransferase	gi|505937406	*D. propionicus*	Sulfur metabolism
SufBD domain protein	gi|330507765	*M. concilii*	Iron-sulfur cluster assembly
Methanogenesis			
5,10-methylene-H4MPT reductase	gi|304314099 gi|1002717 gi|333988092	*Methanobacteriaceae*	Methanogenesis from CO_2
H4MPT S-methyltransferase subunit H	gi|88603421	*M. hungatei*	Methanogenesis from CO_2
Acetyl-CoA decarbonylase/synthase β-subunit	gi|330507407	*M. concilii*	Methanogenesis from acetate
Acetyl-CoA decarbonylase/synthase δ-subunit	gi|330507405	*M. concilii*	Methanogenesis from acetate
Acetyl-CoA decarbonylase/synthase γ-subunit	gi|330507404	*M. concilii*	Methanogenesis from acetate
Methyl-coenzyme M reductase α-	gi|330506955	*M. concilii*	Methanogenesis

subunit			
Methyl-coenzyme M reductase α-subunit	gi|284413655 gi|333988259 gi|284413647 gi|284413653	*Methanobacteriaceae*	Methanogenesis
Methyl-coenzyme M reductase α-subunit	gi|88603395	*M. hungatei*	Methanogenesis
Methyl-coenzyme M reductase β -subunit	gi|330506958	*M. concilii*	Methanogenesis
Methyl-coenzyme M reductase β -subunit	gi|304315297 gi|517427	*Methanothermobacter sp.*	Methanogenesis
Methyl-coenzyme M reductase β -subunit	gi|88603391	*M. hungatei*	Methanogenesis
Methyl-coenzyme M reductase γ -subunit	gi|330506956	*M. concilii*	Methanogenesis
Methyl-coenzyme M reductase γ -subunit	gi|3334251 gi|304315294 gi|209972166	*Methanothermobacter sp.*	Methanogenesis
Coenzyme F420 hydrogenase α-subunit	gi|120503 gi|325957976	*Methanobacterium sp.*	Methanogenesis
Coenzyme F420 hydrogenase β-subunit	gi|330508186	*M. concilii*	Methanogenesis
Energy generation and conservation			
Electron transfer flavoprotein α-subunit	gi|499737807	*S. aciditrophicus*	Electron carrier
Manganese-dependent inorganic pyrophosphatase	gi|330507876	*M. concilii*	Oxidative phosphorylation
V-type ATP synthase α -subunit	gi|330508339	*M. concilii*	Oxidative phopshorylation
V-type ATP synthase β-subunit	gi|330508338	*M. concilii*	Oxidative phopshorylation
Transport & membrane proteins			
ABC transporter substrate-binding protein	gi|330506721	*M. concilii*	Peptides/nickel transport
Extracellular ligand-binding receptor	gi|500019185	*S. fumaroxidans*	Amino acid transport
Extracellular ligand-binding receptor	gi|116696827	*S. fumaroxidans*	Amino acid transport
Extracellular ligand-binding receptor	gi|503306591 gi|502270723	*Variovorax sp.*	Amino acid transport
Periplasmic binding protein	gi|330506714	*M. concilii*	Iron transport system
Periplasmic phosphate-binding protein	gi|503306262 gi|502269613	*Variovorax sp.*	Phosphate transport system
Phosphate binding protein	gi|330508190	*M. concilii*	Phosphate transport system
DNA repair & chaperones			
ATP-dependent DNA helicase	gi|70606034	*Sulfolobus acidocaldarius*	DNA repair
Thermosome	gi|330507490	*M. concilii*	Chaperone
DnaK	gi|499737026	*S. aciditrophicus*	Protein folding
Chaperonin GroEL	gi|501046744 gi|499741908 gi|506415105 gi|501519703	*Anaeromyxobacter sp.*	Protein refolding
Chaperonin GroEL	gi|2493643	*Stenotrophomonas maltophilia*	Protein refolding
Other			
Beta-lactamase domain-containing protein	gi|330506350	*M. concilii*	Xenobiotic degradation
S-layer-related duplication domain-containing protein	gi|330507267	*M. concilii*	Cell envelope
TPR repeat-containing protein	gi|330506457	*M. concilii*	Intracellular traficking and secretion
Hypothetical function			
Hypothetical protein	gi|752801495	*S. fumaroxidans*	Periplasmic transporter protein
Hypothetical protein	gi|330508331	*M. concilii*	Inorganic ion transport and metabolism
Hypothetical protein	gi|330508095	*M. concilii*	Inorganic ion transport and metabolism

Hypothetical protein	gi|330509085	*M. concilii*	Posttranslational modification, chaperones
Phasin family protein	gi|503305728 gi|502268423	*Variovorax sp.*	Unknown function
Pentapeptide repeat-containing protein	gi|330509040	*M. concilii*	Unknown function
Hypothetical protein	gi|330507834	*M. concilii*	Unknown function
Hypothetical protein	gi|330508083	*M. concilii*	Unknown function
Hypothetical protein	gi|330508090	*M. concilii*	Unknown function
Hypothetical protein	gi|88603754	*M. hungatei*	Unknown function
Hypothetical protein	gi|88603509	*M. hungatei*	Unknown function
Hypothetical protein	gi|330508124	*M. concilii*	Unknown function
Hypothetical protein	gi|88602287	*M. hungatei*	Unknown function
Hypothetical protein	gi|494524963	*Methanolinea tarda*	Unknown function
Hypothetical protein	gi|506347166	*V. paradoxus*	Unknown function

FIGURE AND TABLE LEGENDS

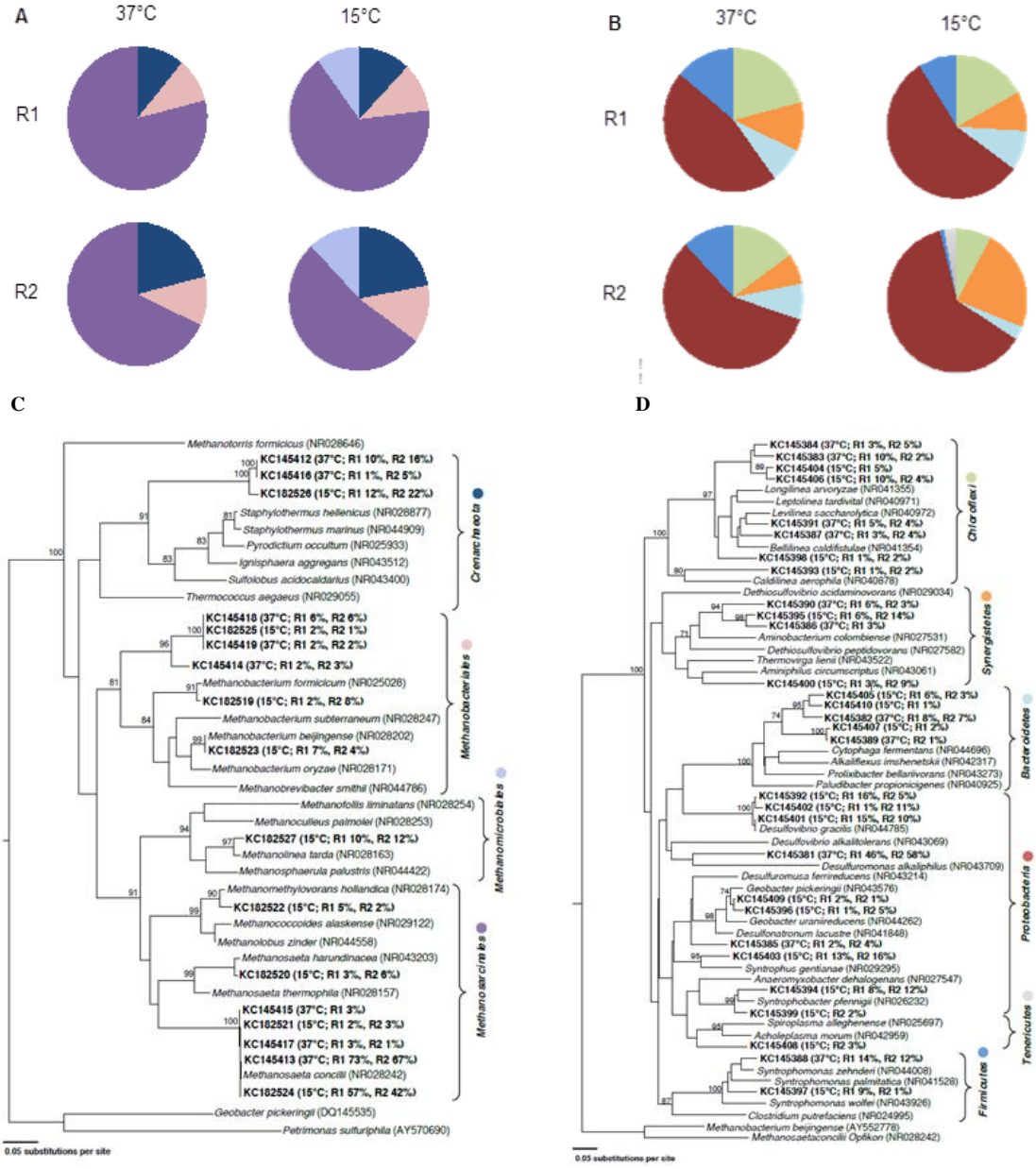

Figure 1. Phylogenetic affiliation of (**A**) archaeal and (**B**) bacterial 16S rRNA gene sequences identified from day 125 (37°C) and day 240 (15°C) bioreactor biomass, calculated using the GTR + gamma model of DNA substitution implemented by RAxML 7.0.3 (Stamatakis, 2006). Bootstrap replicates (total 1000 replicate samples) supporting the branching orders are shown at relevant nodes.

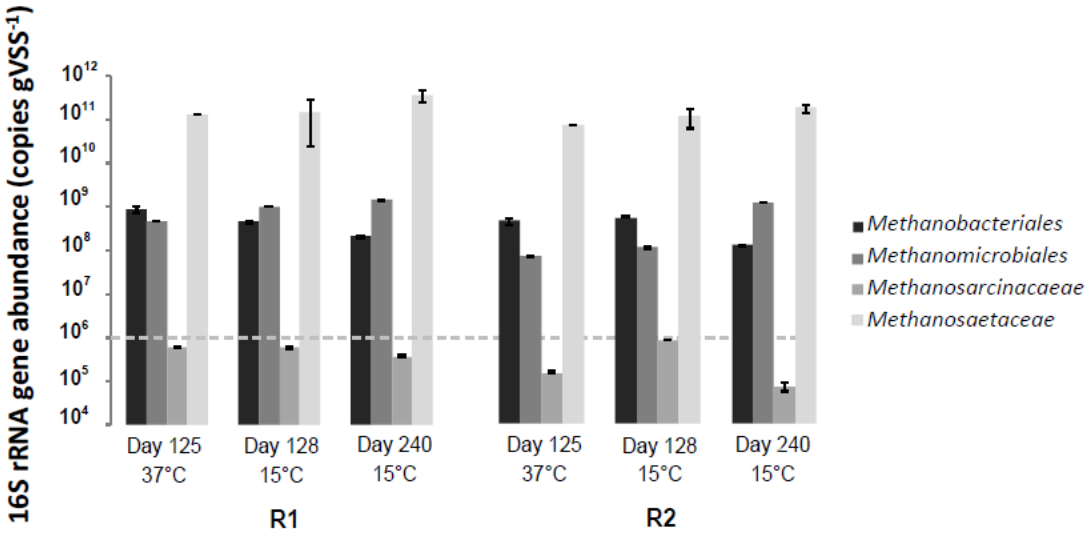

807

808 **Figure 2.** Absolute quantification of the 16S rRNA gene abundance of methanogens

809 from biomass sampled on day 125 (37°C), 128 and 240 (15°C) for R1 and R2

810 bioreactors. Error bars indicate the standard deviation and are the result of two

811 replicates. Dashed line relates to detection limit of assay (10^6 copies $gVSS^{-1}$).

812

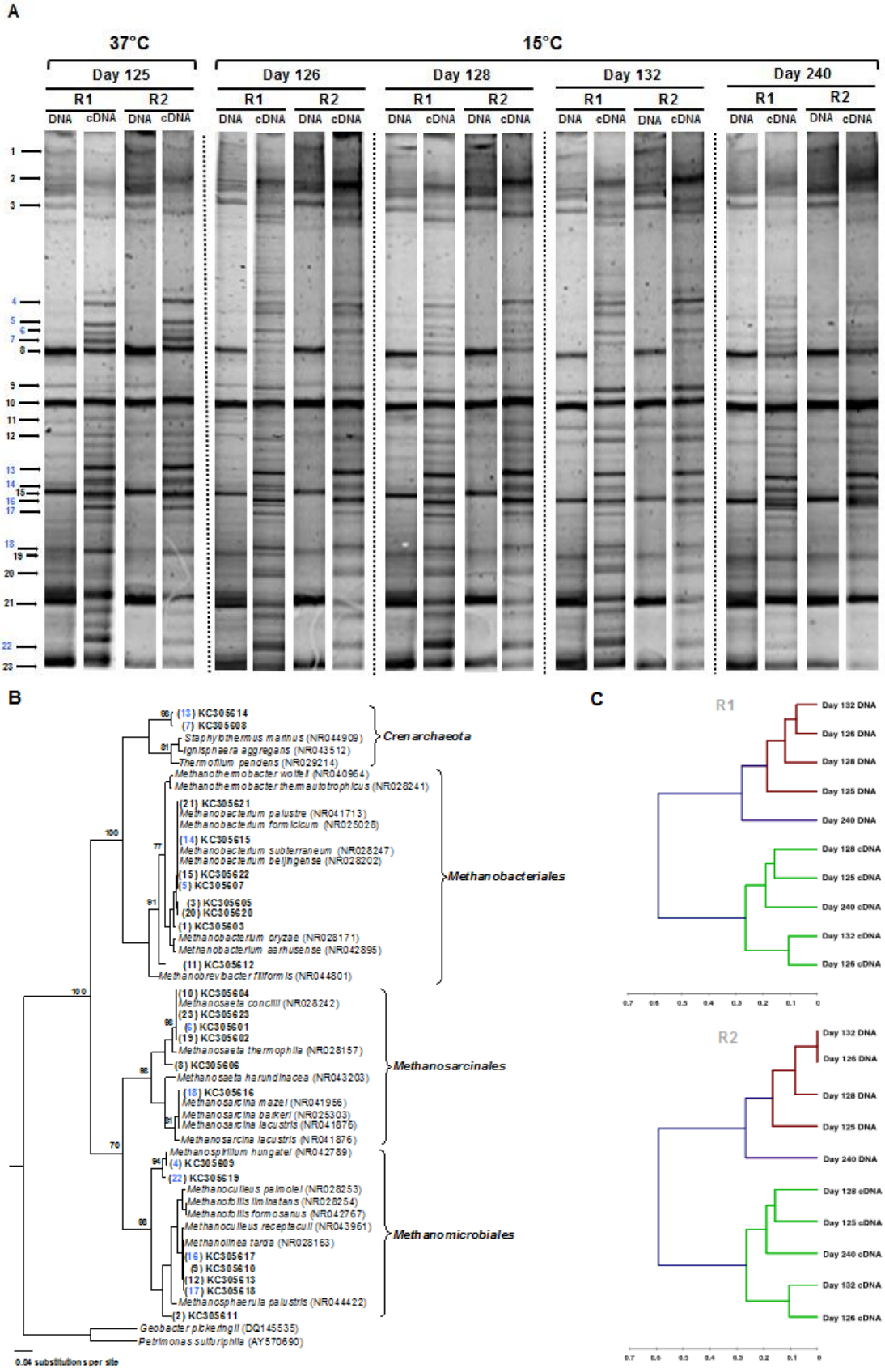

Figure 3. (**A**) 16S rRNA based DGGE analysis of archaea present in R1 and R2 at 37°C (Day 125), initial days after a temperature drop to 15°C (Days 126, 128 and

817 132) and also at the end of trial (Day 240; 15°C). Arrows indicate excised DGGE
818 bands that were sequenced for both R1 and R2. Numbers in blue indicate bands that
819 were more prominent in cDNA than in DNA profiles (**B**) Phylogenetic affiliation of
820 the archaeal 16S rRNA gene sequences obtained from the selected DNA and cDNA
821 DGGE bands, calculated by using a GTR + gamma model of DNA substitution
822 implemented by RAxML 7.0.3 (Stamatakis, 2006). Bootstrap replicates (total 1000
823 replicate samples) supporting the branching order are shown at relevant nodes. DGGE
824 band relating to sequence is in parentheses. **(C)** UPGMA cluster analysis of archaeal
825 16S rRNA gene fragments generated from DGGE profiles. Similarity calculated by
826 Sørensen's (Bray-Curtis) distance measurement.
827

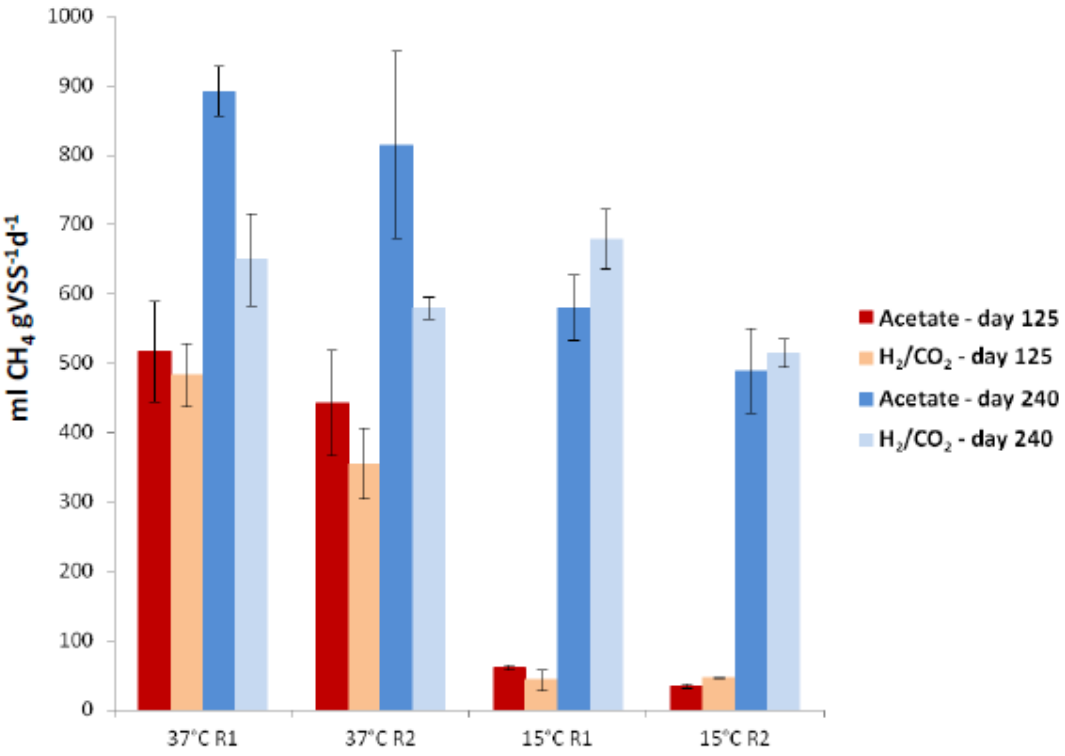

828

829 **Figure 4.** Specific methanogenic activities from biomass sampled on day 125 (37°C)

830 and day 240 (15°C) for direct methanogenic substrates, namely acetate and H_2/CO_2.

831 Results are expressed as ml CH_4 $gVSS^{-1}d^{-1}$. All values are means of triplicate

832 measurements and error bars indicate the standard deviation.

833